BMC Microbiology

RESEARCH

Open Access

Antibacterial efficacy of mycobacteriophages against virulent *Mycobacterium tuberculosis*

Sharumathi Jeyasankar[1], Yeswanth Chakravarthy Kalapala[1], Pallavi Raj Sharma[1] and Rachit Agarwal[1*]

Abstract

Tuberculosis (TB) remains a major global health concern, with drug-resistant strains posing a significant challenge to effective treatment. Bacteriophage (phage) therapy has emerged as a potential alternative to combat antibiotic resistance. In this study, we investigated the efficacy of widely used mycobacteriophages (D29, TM4, DS6A) against *Mycobacterium tuberculosis* (*M. tuberculosis*) under pathophysiological conditions associated with TB, such as low pH and hypoxia. We found that even at low multiplicity of infection (MOI), mycobacteriophages effectively infected *M. tuberculosis*, got rapidly amplified, and lysed *M. tuberculosis*, demonstrating their potential as therapeutic agents. Furthermore, we observed a novel phage tolerance mechanism with bacteria forming aggregates after several days of phage treatment. These aggregates were enriched with biofilm components and metabolically active bacteria. However, no phage tolerance was observed upon treatment with the three-phage mixture, highlighting the dynamic interplay between phages and bacteria and emphasizing the importance of phage cocktails. We also observed that phages were effective in lysing bacteria even under low pH and low oxygen concentrations as well as antibiotic-resistant bacteria. Our results provide key insights into phage infection of slow-growing bacteria and suggest that mycobacteriophages can effectively eliminate *M. tuberculosis* in complex pathophysiological environments like hypoxia and acidic pH. These results can aid in developing targeted phage-based therapies to combat antibiotic-resistant mycobacterial infections.

Keywords Phage therapy, Phage cocktails, Pathophysiological conditions, Low pH, Hypoxia, Multiplicity of infection (MOI), Phage resistance, Drug-resistant tuberculosis

Introduction

Tuberculosis (TB) is one of the oldest recorded human diseases but remains a major life-threatening disease [1]. The WHO estimated that there were 10.6 million new TB cases and 1.3 million TB deaths in 2022 [2]. TB is caused by an airborne pathogen, *Mycobacterium tuberculosis* (*M. tuberculosis*), which has a unique cell wall rich in lipids, that makes it resistant to stains, dyes, and many antibiotics [3]. *M. tuberculosis* resides primarily in the lung interstitium and can replicate within macrophages, forming characteristic granulomas that allow the bacteria to remain dormant for extended periods before becoming active [4]. The pathogen employs various mechanisms to evade host cell defenses, enabling persistent infections. [5–7].

Due to the intricate nature of tuberculosis pathology [8], antibiotic monotherapy is not recommended for tuberculosis treatment. Instead, a combination of multiple antibiotics is used, typically involving a four-drug regimen (isoniazid, rifampicin, ethambutol, and pyrazinamide) for susceptible strains [1]. The emergence of drug-resistant strains challenges TB control. According

*Correspondence:
Rachit Agarwal
rachit@iisc.ac.in
[1]Department of Bioengineering, Indian Institute of Science, Bengaluru, India

to WHO Report 2021, an estimated 450,000 drug-resistant TB cases were reported, with a global treatment success rate of only 60% [3]. The WHO recommends a 6-month treatment plan for multidrug-resistant (MDR) or rifampicin-resistant TB, using bedaquiline, pretomanid, linezolid, and moxifloxacin which has shown an 89% treatment success rate in the TB-PRACTECAL phase 3 trial [9]. However, this regimen's complexity, potential side effects such as peripheral neuropathy [10], and emerging resistance to its components [11–13] highlight the need for alternative treatments.

Phage therapy presents a promising solution for combating antibiotic resistance without harming the host microbiota, offering a precise and effective alternative [14]. Phages are viruses that specifically target bacteria, can be isolated from various sources and have been extensively studied against *M. tuberculosis* [15, 16]. The actinobacteriophage database at PhagesDB.org has around 13,500 phages that infect Mycobacterium species, with 2439 sequenced. These phages are diverse and have been classified into several clusters and subclusters. Several of these phages are initially isolated from *M. smegmatis* with only a subset known to infect *M. tuberculosis*, especially those that belong to Cluster K and three subclusters (A1, A2, and A3) of Cluster A [17, 18].

Several studies have explored the potential of phage therapy against TB. Carrigy et al. demonstrated that preexposure prophylactic pulmonary delivery of aerosolized mycobacteriophage D29 significantly reduced *M. tuberculosis* burden in mouse lungs, suggesting a valuable intervention for at-risk individuals [19, 20]. Broxmeyer et al. employed *Mycobacterium smegmatis*, a non-virulent strain, to deliver the lytic phage TM4 within RAW 264.7 macrophages infected with *M. avium* and *M. tuberculosis* individually, showing a reduction in viable intracellular bacteria [21]. Guerrero-Bustamante et al. engineered a bacteriophage cocktail comprising five phages (AdephagiaΔ41Δ43, Fred313_cpmΔ33, FionnbharthΔ45Δ47, Muddy_HRMN0157-1 (gp24 G487W), and D29), to minimize the emergence of resistance and efficiently eliminate the tested *M. tuberculosis* strains without compromising antibiotic effectiveness [16]. Yang et al. demonstrated that bacteriophage strains D29 and DS6A effectively lysed *M. tuberculosis* in vitro and improved health outcomes in humanized mice infected with *M. tuberculosis* [22].Furthermore, in clinical settings, mycobacteriophages have demonstrated effectiveness in treating various mycobacterial infections, particularly against *Mycobacterium abscessus* [23–26].

Despite these promising findings, the application of phage therapy for TB treatment faces significant physiological challenges, such as the formation of granulomas in the lungs, characterized by hypoxia, nutrient deprivation, and acidic microenvironments [27, 28]. A deeper understanding of phage-bacterial dynamics under these conditions is crucial for developing effective phage therapies. While previous research in our laboratory explored the effectiveness of phages against *M. smegmatis* [29], the phage-bacterial dynamics of slow-growing *M. tuberculosis* in various pathophysiological environments remain unexplored. Therefore, it is crucial to study how phages perform under both normal physiological conditions and the challenging pathophysiological environments typical of bacterial infections.

In this study, we investigate the interaction dynamics between phages and *M. tuberculosis* in different pathophysiological conditions associated with TB, including low pH and hypoxia. Additionally, we conducted prolonged period testing and evaluated efficacy in antibiotic-resistant strains. We also examined the development of phage tolerance and resistance in *M. tuberculosis*. Overall, our results suggest that phages can rapidly amplify and efficiently eliminate the slow-growing pathogen in physiological environments and in low pH and hypoxia. These findings significantly contribute to our understanding of phage infection dynamics in slow-growing bacteria and aid in developing phage therapies to combat antibiotic-resistant mycobacterial infections.

Materials and methods

Bacterial cell culture and maintenance

Experiments involving *Mycobacterium tuberculosis* H37Rv (a kind gift from Prof. Amit Singh, Indian Institute of Science, Bengaluru, India) were performed in a Biosafety level – 3 (BSL-3) facility (Institutional Biosafety Committee approval: IBSC/IISc/RA/20/2020). Primary cultures of *M. tuberculosis* H37Rv were grown in Middlebrook 7H9 broth supplemented with 0.2% glycerol, 10% OADC (Bovine albumin fraction V 2.5 g, Dextrose 1 g, Catalase 0.0015 g, Oleic acid 0.025 g in 50 mL distilled water), and 0.05% Tween-80. A log-phase primary culture was inoculated into a secondary culture without Tween-80 and supplemented with 2 mM Calcium Chloride ($CaCl_2$) to promote efficient phage infection. All cultures were incubated at 37 °C with rotary shaking at 180 rpm. To measure optical density (OD), 100 µL of bacterial culture at various time points was diluted 10-fold in medium and briefly sonicated for 15 s to obtain a uniform cell suspension. Readings were taken using a spectrophotometer (Jenway 7205 UV/Visible Spectrophotometer) at 600 nm against a media blank.

Preparation of phage: phage amplification and maintenance

D29 and TM4 mycobacteriophages were amplified using *M. smegmatis*, while DS6A was amplified using *M. tuberculosis H37Rv*. The soft agarose overlay technique was used to amplify and quantify phages. Initially,

soft agarose was prepared by adding agarose (0.6% final concentration) to 7H9 media supplemented with 2 mM $CaCl_2$. After autoclaving, the suspension was allowed to cool down to 42 °C, and a log-phase culture of the respective bacterial strain (OD 1–2) was added. The soft agarose suspension was poured into the plates containing solidified media composed of 1.5% agarose and 7H9 media with necessary supplements.

The phage sample (at an MOI of 10) was spotted on top of the soft agarose. The plates were then incubated at 37 °C for 12–24 h for *M. smegmatis* and 12–14 days for *M. tuberculosis* H37Rv. After incubation, to facilitate diffusion, an appropriate amount of Magnesium Sulfate-Tris Chloride-Sodium Chloride Buffer (SM Buffer) was added to the soft agarose. The plate was further incubated for 3–4 h at 37 °C or overnight at 4 °C. Plates were incubated upright, allowing the condensation of water droplets on the lids. The water droplets help to disperse phage across the bacterial lawn as they fall from the lid [30]. Afterward, the soft agarose and the water droplets on the lid were collected in a 50mL falcon and centrifuged at 4,000 g for 10 min at 4° C. The supernatant was collected and filtered using 0.22 µm syringe filters. The soft agarose overlay was utilized to determine the phage titers.

The phage titers were verified by spot assays. Mid-log phase *M. smegmatis* cultures or *M. tuberculosis* (OD > 1) were plated on Middlebrook 7H9 media supplemented with 1.5% agarose, CaCl2 (2 mM), 10% OADC, and 0.2% glycerol to form a bacterial lawn. Serial dilutions of the phage samples were then spotted on the bacterial lawn. The plates were incubated at 37 °C for 24 h for *M. smegmatis* or 6–7 days for *M. tuberculosis*, and subsequently, the number of plaques formed at various dilutions were counted.

Bacterial growth kinetics

To study the bacterial growth kinetics, 7H9 broth was supplemented with 10% OADC and 2 mM $CaCl_2$. This medium was then inoculated with 150 µL of a log-phase secondary bacterial culture with an optical density (OD) of 1–2 per 10 mL of the media. The cultures were incubated at 37°C with rotary shaking at 180 rpm. Periodic measurements of bacterial optical density (OD) were taken. For phage-treated samples, different MOIs of each phage or 2-phage mixtures (D29 and TM4, D29 and DS6A, TM4 and DS6A) at 1 MOI or 3-phage mixture (D29, TM4, and DS6A) were added in their respective culture tubes, at the appropriate time, either at the start of the experiment during the lag phase or at a specified interval during the mid-log phase.

SEM imaging

Scanning electron microscopy (SEM) (ThermoFisher XL – 30 ESEM) of the bacterial aggregates was carried out to examine the morphology of the samples. The bacterial aggregates were pelleted at 1000 *g* and resuspended in 500 µL of PBS. The samples were fixed by adding 4% paraformaldehyde (final concentration). 20 µL of the sample was evenly applied onto a double-sided carbon tape placed on a metal stub and vacuum dried, followed by sputter coating with gold (20 nm) and rastered using an electron beam (15 keV).

HADA labeling and confocal imaging

To label the actively growing bacteria [31, 32], we introduced a final concentration of 0.1 mM of HADA (3-[7-hydroxycoumarin]-carboxamide-D-Alanine) (R&D Systems) into 1 mL of a TM4 phage treated culture having aggregated bacterial regrowth and allowed it to incubate for 3 h. Subsequently, the cells were subjected to two washes in 7H9 medium and fixed by adding 4% paraformaldehyde (final concentration). Agarose pads were created on coverslips to facilitate imaging by evenly spreading 1% agarose. The prepared cell sample was then applied to the agarose pad and dried. These coverslips were subsequently mounted onto an imaging dish and securely sealed. Image acquisition was performed utilizing a Leica SP8 confocal microscope, employing a 63x magnification objective lens with oil immersion. The acquired images were further processed and analyzed using ImageJ software for subsequent evaluation and data extraction.

Enzymatic treatment of bacterial aggregates

Bacterial aggregates were individually treated with Cellulase (5 mg/mL in citrate buffer) for 6 h, or DNase-1 (0.8 U/mL) for 9 h, or Proteinase K (0.1 mg/mL) for 6 h, at 37 °C respectively. Additionally, a sequential combined treatment was performed where aggregates were first treated with Cellulase (5 mg/mL in citrate buffer) for 6 h, followed by DNase-1 (0.8 U/mL) for 9 h, and then Proteinase K (0.1 mg/mL) for 6 h, all at 37 °C, with washing between each step. Following the enzymatic treatments, the aggregates were thoroughly washed thrice with PBS to remove any residual enzymes and buffers. Subsequently, 1 mL of a 1% crystal violet solution was added to each sample and incubated for 10 min at 37° C. After this incubation period, cultures were washed three times with 1X PBS and then incubated with 1 mL of 95% ethanol for 10 min to extract the crystal violet dye. The absorbance of the dye was measured at 650 nm.

Calcofluor white staining

The bacterial aggregates and planktonic bacteria were positioned on glass slides. A drop of Calcofluor white (CW) was applied directly onto the samples, followed by the addition of a drop of 10% KOH. A coverslip was then gently placed over the samples, and imaging was

performed using an upright microscope under oil immersion at 100X magnification. The Calcofluor white signal was captured at 460 nm emission, utilizing the DAPI channel [33].

Bacterial growth kinetics with phage – pH and hypoxia

To investigate the impact of acidic pH on phage infection dynamics, we conducted a phage kinetics assay under pH 5 following a previously described method [34]. Bacterial cultures were grown to the mid-log phase in 7H9 media, followed by two washes in phosphate-buffered saline. Subsequently, these cultures were introduced into 7H9 media, adjusted to a pH of 5.0, and supplemented with 2 mM $CaCl_2$. The pH was then maintained using MES (2-(N-Morpholino) ethanesulfonic acid) (HiMedia) buffer at a concentration of 100 mM. To this medium, 50 µL of 40 mM oleic acid (OA) and 10 µL of 100 mM cholesterol (dissolved in ethanol: tyloxapol at 1:1) were added every two days. The cultures were then allowed to grow under acidic pH conditions for seven days. After this acid treatment, the cultures were washed with 7H9 at pH 5 to remove accumulated tyloxapol. Subsequently, the culture was inoculated at a concentration of 1×10^7 colony-forming units (CFU)/mL (OD_{600}: 0.1) in 7H9 media with a pH of 5.0. For the groups treated with phages, a three-phage cocktail was introduced at a MOI of 1. Bacterial growth was monitored over 14 days using CFU assays. At specific time points, serial dilutions of the cultures were prepared in PBS and plated onto 7H11 solid agar plates containing glycerol and OADC supplements, followed by incubation at 37 °C for 3–5 weeks to assess bacterial growth.

To investigate the efficiency of phage infection during hypoxia, the cultures were grown within plastic Silicone-coated Vacutainers (BD Cat No. 367820) to create hypoxic conditions. Briefly, bacterial cultures with an optical density (OD_{600}) of 0.1 were prepared in 7H9 medium, supplemented with Glycerol, ADC, Calcium Chloride (2 mM), and 1.5 µg/mL of methylene blue. These cultures were then aseptically injected into the BD Vacutainers using a 26 G needle. Subsequently, samples were collected using a syringe and a 20 G needle for spectrophotometer readings and CFU (colony-forming unit) assays. Oxygen levels were tracked by measuring the optical density of Methylene Blue at 665 nm. For groups subjected to phage treatment, a three-phage cocktail was administered at a multiplicity of infection (MOI) of 1, either at the experiment's onset during the lag phase or when methylene blue indicated the onset of hypoxia [35, 36].

Antibiotic growth kinetics

To investigate the combined effects of antibiotics (specifically, isoniazid or rifampicin) and phage treatment on *M. tuberculosis* H37Rv growth, 7H9 broth supplemented with ADC and 2mM $CaCl_2$ were prepared and inoculated with 100 µL of log phase secondary bacterial culture per 10 mL of the media. The cultures were then incubated at 37 °C with rotary shaking at 180 rpm. For antibiotic-treated samples, a final concentration of rifampicin at 2 µg/mL and isoniazid at 10 µg/mL were added at the appropriate time (either at the lag phase or at a specified interval of the mid-log phase). Similarly, a three-phage cocktail was added at 0.0001 MOI for phage-treated samples at lag and log phase. We co-treated cultures with antibiotics and phages at specified concentrations and phases to assess their combined impact. Optical density (OD) was periodically measured at 600 nm against a blank medium, and a CFU assay was performed to study bacterial growth.

Phage kinetics against isoniazid and rifampicin resistant *M. tuberculosis* Rv $mc^2$8251 (BSL2 strain)

To investigate the impact of a phage cocktail on an antibiotic-resistant strain *M. tuberculosis* Rv $mc^2$8251, we prepared a 7H9 broth supplemented with OADC, $CaCl_2$, and PLAM(L-pantothenate, 24 mg/L; L-leucine, 50 mg/L; L-arginine, 200 mg/L; and L-methionine, 50 mg/L), *M. tuberculosis* Rv $mc^2$8251 [37]. This medium was then inoculated with 100 µL of a log-phase primary bacterial culture of *M. tuberculosis* Rv $mc^2$8251 per 10 mL of media. The cultures were subsequently incubated at 37 °C with rotary shaking at 180 rpm. For the phage-treated samples, a three-phage cocktail was added at MOI of 1 at a specific time, either during the lag phase or at a specified interval during the mid-log phase. For phage-treated samples in the presence of antibiotics, Isoniazid (INH) at 1 mg/L and Rifampicin (RIF) at 4 mg/L concentrations were added, either during the lag phase or at a specified interval during the mid-log phase. At periodic intervals, bacterial optical densities (OD) were recorded using a spectrophotometer at 600 nm against a media blank.

Phage rechallenge experiments

To evaluate the susceptibility of a growing bacterial population to phages after exposure, we determined the titers of our phage stocks on the phage-exposed bacteria. Bacterial cultures that showed growth post-phage treatment (using D29, TM4, DS6A, and a three-phage cocktail) were centrifuged at 1000 *g* for 1 min. The resulting pellet (aggregated bacteria) and the planktonic bacteria (supernatant) were streaked, and single colonies were selected and inoculated in 7H9 media containing OADC, glycerol, and $CaCl_2$. Each phage culture was added to soft agarose and plated on the 7H11 plate. Serial dilutions of the phage stocks were prepared, and the corresponding phage was spotted on the bacterial lawn. The plates were subsequently incubated at 37 °C for 7–10 days, and the number of plaques was counted.

Statistics

All experiments were performed on independent biological replicates. Statistical significance was determined for the control and experimental groups using 2-way ANOVA with Tukey's multiple comparisons test (alpha = 0.05) or one-way ANOVA with Dunnett multiple comparison test, as specified. GraphPad (Prism) was used for all statistical analysis.

Results

Mycobacteriophages reduce bacterial growth in *M. tuberculosis*

To determine the efficacy of bacteriophages in lysing virulent *M. tuberculosis* H37Rv, we amplified three lytic mycobacteriophages, namely D29 (Cluster A), TM4 (Cluster K), and DS6A (Singleton) [PhagesDB.org], each from distinct clusters to titers of 10^{10}. We first conducted infection experiments using *M. tuberculosis* bacterial cultures with D29 and TM4 mycobacteriophages at multiplicities of infection (MOIs) ranging from 1 to 300 at different growth phases (lag and log) (Figs S1 and S2). Significant reductions in optical density (OD) and colony-forming units (CFUs) were observed after 48 h when phages were added during the log phase. No increase in OD was observed in the lag phase phage-treated cultures. The study was conducted for 25 days, and no visible growth was observed during the entire study period after phage infection in both the lag and log phases. To find the minimum MOI at which the phages were effective, we conducted infection studies at lower MOIs. MOIs of 1 and 10^{-2} showed significant growth reduction in both lag and log phases, while MOIs of 10^{-4} and 10^{-6} resulted in reduced culture optical density only when added during the lag phase (Fig S3). Consequently, MOIs of 0.1, 0.01, and 0.001 were selected to study the dynamics between individual mycobacteriophages and *M. tuberculosis* H37Rv. All three phages (D29, TM4, DS6A) individually led to significant growth reduction in CFU and optical density at the MOIs of 0.1, 0.01, and 0.001 (Fig. 1). The CFU and OD were monitored for 58 days as the control CFU dropped significantly after 58 days. To gain insight into why the phages remained effective at consistent levels across different MOIs, we conducted a phage burst experiment to investigate the dynamics of phage replication and release within the *M. tuberculosis* H37Rv cultures. D29 phage was infected at 1 MOI, and the plaque forming unit (PFU) assay was performed regularly to determine the number of phages. We observed a log$_{10}$fold increase in phage numbers within 3–4 h of infection. This implies that the burst time for D29 phage is around 3–4 h in *M. tuberculosis* (Fig S4), much faster than the bacterial replication time of around 24 h. This

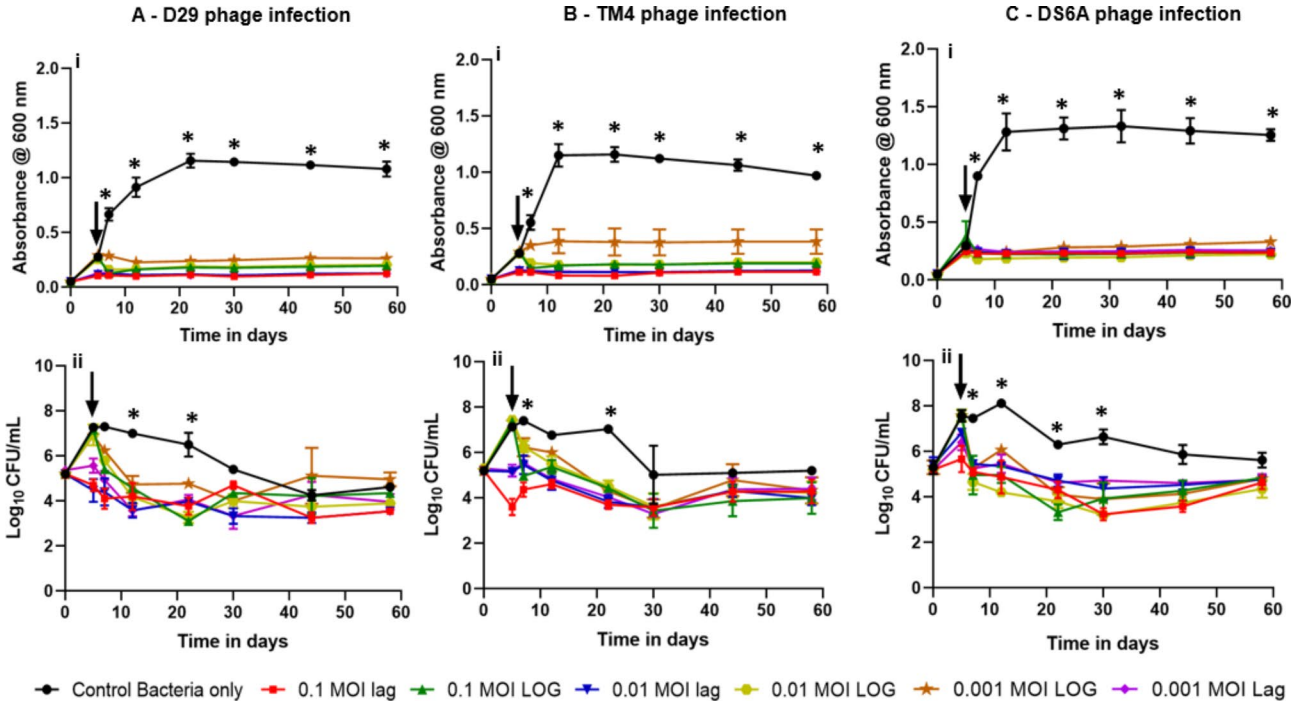

Fig. 1 Efficacy of infection of mycobacteriophage on *M. tuberculosis* H37Rv. Growth curves of *M. tuberculosis* in liquid culture in the presence of (**A**) D29, (**B**) TM4, and (**C**) DS6A phage. The study includes **(i)** Measurements of culture absorbance at 600 nm over time and **(ii)** Colony Forming Unit (CFU) measurements over time. The black arrow represents the time when phage solution was added to the cultures. These experiments were repeated several times (≥ 2) (with $n = 3$), and the representative graphs were plotted. 2-way ANOVA with Tukey's multiple comparisons test was used to determine statistical significance ($p < 0.05$). * Indicates a significant difference ($p < 0.05$) between the control and all phage groups at that time point.

could explain effectiveness at low MOIs as the phages can build up their numbers and reach high MOI before bacteria can replicate.

Bacterial regrowth after phage infection was observed as tiny clumps with clear supernatant in all single phage-treated cultures, with varying regrowth times. D29 and TM4-treated cultures exhibited regrowth at around 110 days, while DS6A-treated cultures showed regrowth at around 75 days. These regrowth times were noted based on visual observations of tiny clumps in the culture tubes (Fig S5), as the OD readings did not change due to the clear supernatant. No significant differences were observed in bacterial regrowth patterns with varying MOIs. The regrowing bacteria formed aggregated clusters, and as time progressed, these clusters increased in size. Surprisingly, we did not observe any increase in the planktonic OD. We determined phage titers to evaluate the stability and activity of the phages during this regrowth phase. The results showed that active phages were present in the media even after several months after inoculation (Table S1). To test whether this regrowing bacterium is genetically resistant to the phage, for each phage-treated group, we collected the aggregates, resuspended them in 1 mL of fresh media and streaked them onto separate 7H11 agar plates. Subsequently, five single colonies were selected from each plate and inoculated in the fresh liquid medium. Phage infection efficiency was checked by conducting a PFU assay with the respective phage on the regrown bacterial culture. We found that bacteria were not genetically resistant as phages could infect the bacteria at the same efficiency as the control bacteria (Table S2).

Our investigation revealed that the bacteria displayed no genetic resistance, as phages could infect them with the same efficiency as the control bacteria. To further explore the phenotype of these bacterial aggregates, we employed Scanning Electron Microscopy (SEM) imaging, as depicted in Fig. 2A. The SEM images showed a densely packed biofilm-like morphology within the aggregates, devoid of visible pores. We conducted HADA staining to confirm the presence of bacteria within the aggregates and assess their metabolic activity. HADA, functioning as an amino acid alanine analog, is incorporated in peptidoglycan during its synthesis, a process intricately dependent on alanine incorporation. This facilitates visualization of actively metabolizing bacteria within the aggregates. Subsequently, to capture these aggregates in three dimensions, we utilized Z-stack imaging through confocal microscopy (Fig. 2B). Our findings confirmed that the HADA staining signals were indeed localized within the aggregates in the form of rod-shaped bacteria, providing evidence of active bacterial metabolism. To test the composition of the aggregates, we stained some of these aggregates for cellulose through calcofluor white staining (Fig. 2C). The aggregates showed a strong signal for cellulose, indicating the presence of cellulose in aggregates.

Furthermore, when these aggregates were treated with DNase, Proteinase K, and Cellulase, a reduction in crystal violet optical density was observed (Fig. 2D). Crystal violet has a strong affinity to extracellular polymeric substances and is a widely utilized indicator for biofilm estimation [38]. The observed reduction in optical density (OD) following enzyme digestion is attributable to the high concentration of polymeric substances - DNA, protein, and cellulose, within the aggregates. This supports the hypothesis that these substances play a crucial role in aggregates and serve as a strategic adaptation by bacteria to exclude phage interaction with the bacterial surface receptor.

Phage cocktails show synergy in growth reduction

Since phages worked well at low MOIs and high phage MOIs can result in lysis from without [39, 40], we chose to use the MOI of 1 for all subsequent assays. To test the effect of phage cocktails, *M. tuberculosis* H37Rv cultures were exposed to different combinations of phages. These included a cocktail of 3 phages (D29, TM4, and DS6A) and various 2-phage cocktails, such as D29 and TM4, D29 and DS6A, and DS6A and TM4, at 1 MOI. Phage cocktail treatment significantly reduced the optical density and CFU of the bacterial cultures. Like the single phage-treated cultures, bacteria started to regrow in all two phage-treated groups at around 65 days after phage treatment (Fig. 3A). The regrowth looked like tiny clumps with clear supernatant as observed with all single phage-treated cultures. These were also noted based on visual observations of tiny clumps in the culture tubes, as the OD readings did not change due to the clear supernatant.

For the three-phage treated cultures, bacterial regrowth was not observed for up to 100 days (Fig. 3B (i)). CFUs were also below the detection limit after a month of treatment (Fig. 3B (ii)). This shows that the cocktail of phages can act synergistically to lyse the bacteria and prevent the regrowth of bacteria for a longer time. This three-phage cocktail at MOI of 1 was used for all subsequent experiments.

Mycobacteriophages are effective under low pH and hypoxia

To assess the efficacy of phage infection under pathophysiological conditions, we cultured the bacteria in two distinct settings. First, we subjected them to hypoxic conditions using vacutainers, reaching a hypoxic state at approximately day 12 of the experimental setup, as evidenced by the decreased methylene blue readings [35, 36] (Fig. 4A (i) and (ii)). Notably, in both phage-treated groups (before and after the onset of hypoxia), several

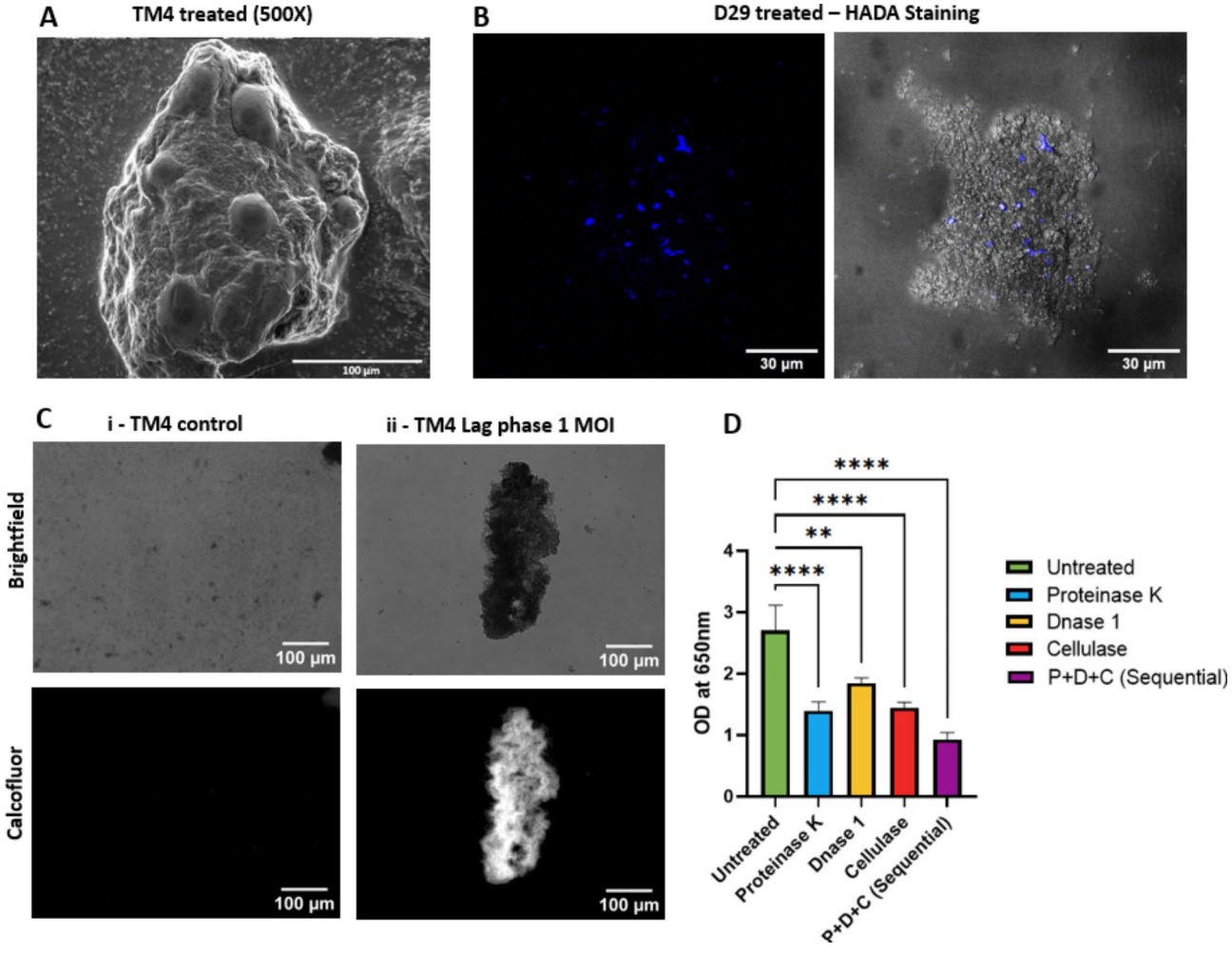

Fig. 2 Characterization of aggregated bacterial regrowth. (**A**) Representative SEM image of TM4 phage treated bacterial aggregate (at 500X magnification), (**B**) Representative image of HADA incorporation in the bacteria in the aggregate (Excitation/Emission, λ: ~405/450 nm; Scale: 30 µm) (**C**) Image of Cellulose and Calcofluor staining on the aggregates; **i** – Control bacteria, **ii** – TM4 phage treated at 1 MOI Lag phase bacteria (Scale: 100 µm). (**D**) Proteinase K (P), DNase (D), and Cellulase (C) treatment on the aggregates. One-way ANOVA with the Dunnett multiple comparisons test was used to determine statistical significance ($p < 0.05$). * Indicates the level of significant difference ($p < 0.05$) between the untreated and the respective enzyme-treated groups.

log order reductions in colony-forming units (CFU) were observed within 48 h of phage introduction (Fig. 4A (iii)).

To study the efficiency of phage infection in an acidic environment, we tested the stability of these phages at pH 5 and found them to be stable (Fig S6). We exposed the bacteria to a low pH environment (pH 5) with host-relevant carbon sources (oleic acid and cholesterol) [34] for seven days before introducing phages. Following phage administration, we observed a significant CFU reduction (4-log order) within seven days (Fig. 4B).

Testing synergy between mycobacteriophages and antibiotics

To assess the effectiveness of bacteriophages in lysing antibiotic-treated *M. tuberculosis* and explore the potential synergy between phages and antibiotics, we conducted a phage kinetics study in the presence of antibiotics in the culture. We selected rifampicin at 2 mg/L or isoniazid at 10 mg/L, concentrations that demonstrated substantial effectiveness during the lag phase but lacked efficacy during the log phase (Fig S7).

Upon the simultaneous introduction of phages (3-phage mixture at 0.0001 MOI) and isoniazid (10 mg/L) during the lag phase, their effectiveness mirrored that of phages alone. Notably, only the isoniazid-treated groups exhibited regrowth after 15 days. In contrast, the cultures where both isoniazid and phages were treated simultaneously, like those treated with phages alone, did not regrow during the treatment period (Fig. 5A(i)). This suggests that phages were effective when added with isoniazid during the lag phase.

However, when introduced during the log phase, although notably effective compared to the control, the combined impact of phages and isoniazid was similar to

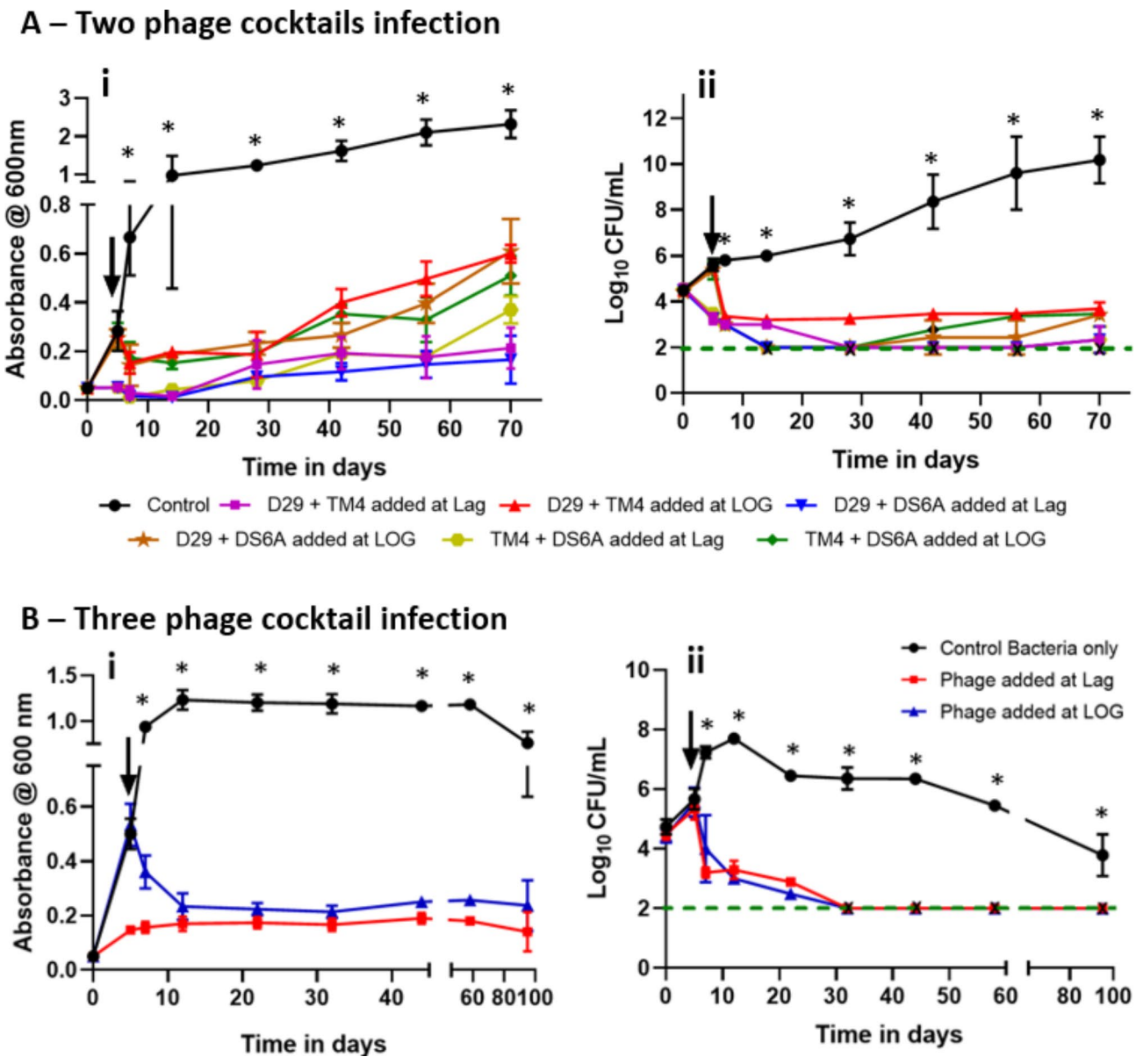

Fig. 3 Phage cocktails show synergy and are more effective against *M. tuberculosis* than single phage. **(A)** Growth curves of *M. tuberculosis* in presence of 2-phage cocktail (D29 + TM4, D29 + DS6A, DS6A + TM4) at 1 MOI **(B)** Growth curves of *M. tuberculosis* in the presence of 3-phage cocktail (D29, TM4, and DS6A) at 1 MOI, where **(i)** Measurements of culture absorbance at 600 nm over time, and **(ii)** Colony Forming Unit (CFU) measurements over time. The black arrow represents the time when phage solution was added to the cultures. The dashed green line indicates the limit of detection. 2-phage cocktail with D29 and TM4 and 3-phage cocktail experiments were repeated twice (with $n = 3$), and the representative graphs were plotted. 2-way ANOVA with Tukey's multiple comparisons test was used to determine statistical significance ($p < 0.05$). * Indicates a significant difference ($p < 0.05$) between the control and phage groups between 10 and 95 days for absorbance vs. time and from day 7 for Log_{10} CFU/mL vs. time.

the isoniazid alone. It did not surpass that of phages acting alone in reducing bacterial numbers (Fig. 5A(ii)). This implies a lack of synergy between phages and isoniazid during the log phase.

Similarly, for cultures co-treated with rifampicin (2 mg/L) and phages (3-phage mixture at 0.0001 MOI), significant effectiveness was observed compared to the control. Yet, it did not surpass the impact of phages alone in reducing the bacterial numbers after treatment of both lag and log phases (Fig. 5B (ii)), further emphasizing the absence of synergy between phages and rifampicin. This suggests that the phage and antibiotic co-treatment performed similarly to or better than only antibiotics; however, the co-treatment resulted in a worse outcome compared to phage alone, suggesting a lack of synergy.

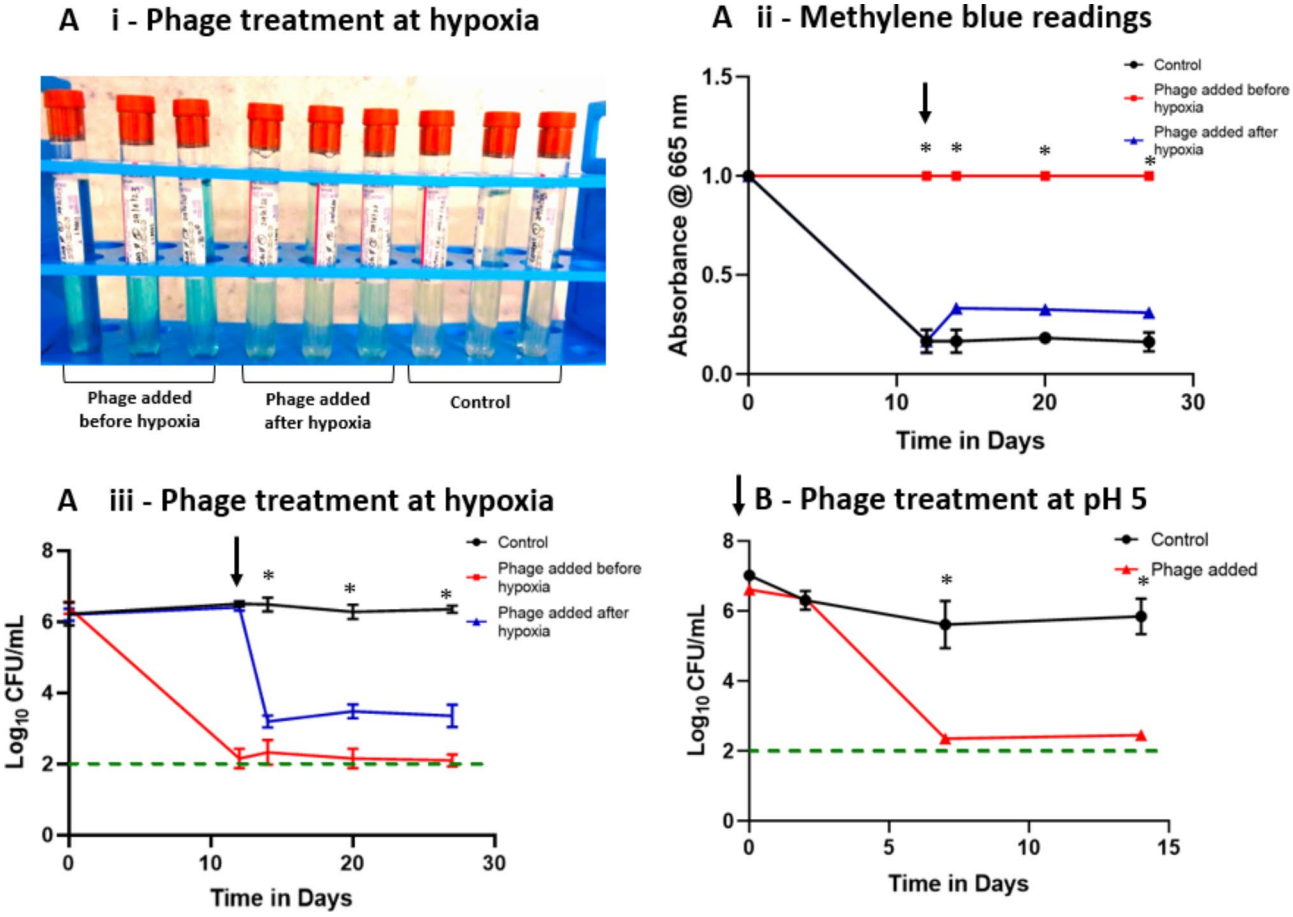

Fig. 4 Mycobacteriophages are effective under various pathophysiological conditions. Growth kinetics of *M. tuberculosis* H37Rv cultures treated with a three-phage cocktail at (**A**) hypoxic condition, where (**i**) represents a photograph of vacutainers of all treatment groups after phage treatment, (**ii**) represents methylene blue readings at 665 nm, and (**iii**) represents $\log_{10}$CFU/mL vs. time, and (**B**) pH condition of 5. The black arrow represents the time when phage solution was added to the cultures. The dashed green line indicates the limit of detection. These experiments were repeated twice (with $n = 3$), and the representative graphs are shown here. 2-way ANOVA with Tukey's multiple comparisons test was used to determine statistical significance ($p < 0.05$). * Indicates a significant difference ($p < 0.05$) between the control and phage groups.

Mycobacteriophages are effective against drug-resistant *M. tuberculosis*

Both Rifampicin and Isoniazid-resistant infections are on the rise [9]. Hence, we, tested the efficacy of mycobacteriophages against *M. tuberculosis* $mc^2$8251, which is both rifampicin and isoniazid-resistant strain [37]. We conducted the infection experiment with a three-phage cocktail at 1 MOI. The OD readings were taken periodically (Fig. 6A). We observed that the three-phage cocktail effectively infects and lyses antibiotic-resistant *M. tuberculosis* $mc^2$8251, and no regrowth was observed for up to 150 days.

We then tested whether the phages would remain effective in the presence of both rifampicin and isoniazid. For this, we treated cultures with isoniazid at 1 mg/L, rifampicin at 4 mg/L, below their minimum inhibitory concentrations for this strain [37], and a simultaneous three-phage cocktail at 1 MOI. Surprisingly, unlike the antibiotic and phage combined treatment against *M. tuberculosis* H37Rv (Fig. 5), the phages demonstrated effectiveness against *M. tuberculosis* $mc^2$8251 (Fig. 6B) comparable to when they were treated alone (Fig. 6A) at both lag and log phase. These results suggest that phages effectively combat antibiotic-resistant infection and prevent bacterial regrowth.

Discussion

Due to the increasing prevalence of mycobacterial infections and drug-resistant bacteria, particularly multidrug-resistant tuberculosis and extensively drug-resistant tuberculosis [41, 42], it has become crucial to find new methods to control and treat TB.

Although mycobacteriophages have not yet been tested clinically on humans for the treatment of tuberculosis, many studies have reported using phages to treat *Mycobacterium abcessus* infection [23–26]. For instance, successful treatment of a 15-year-old patient with cystic fibrosis and disseminated, antibiotic-resistant

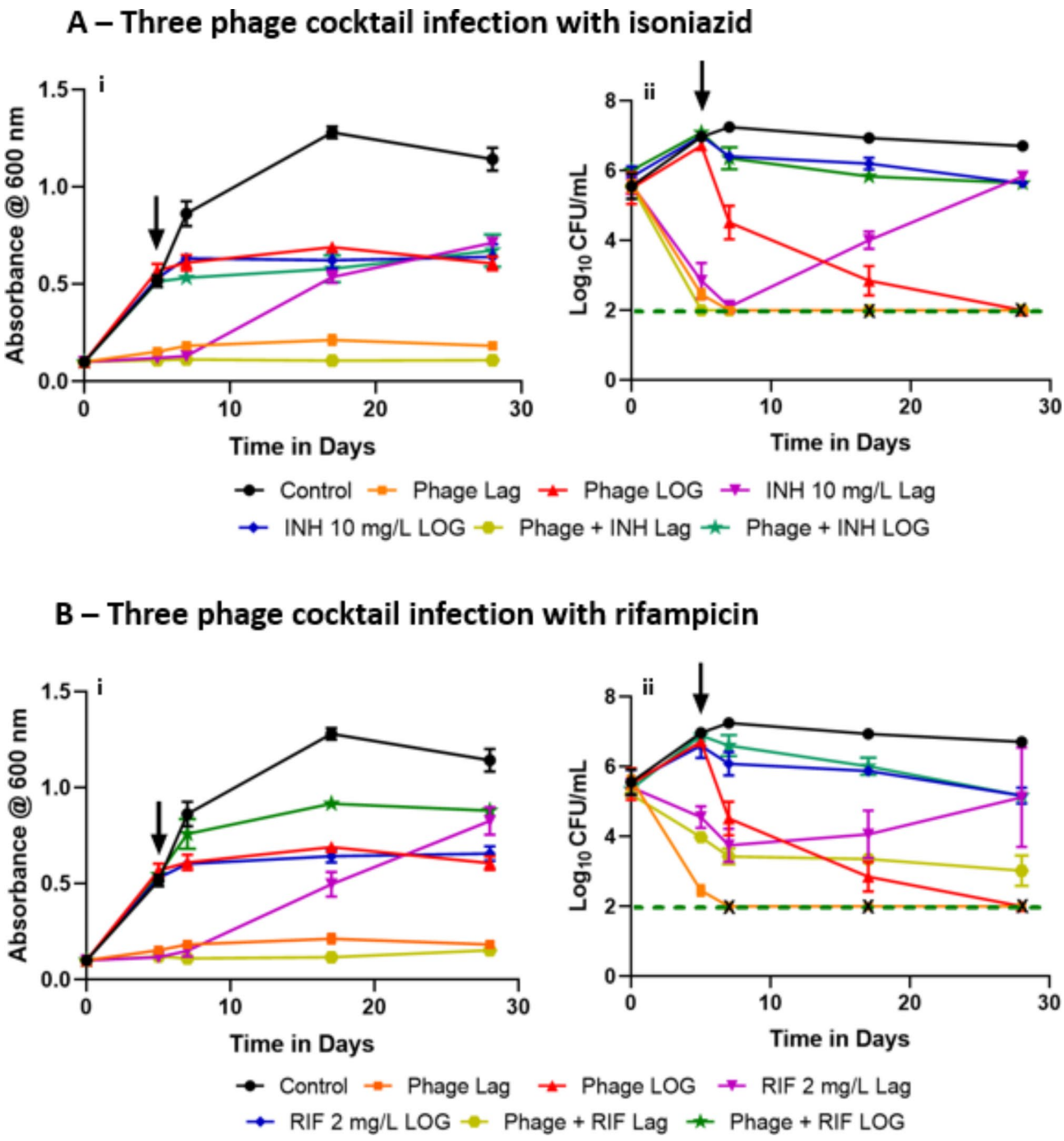

Fig. 5 Combined effect of Mycobacteriophages and Phage cocktail at 0.0001 MOI Growth kinetics of *M. tuberculosis* H37Rv cultures treated with **(A)** the 3-phage cocktail at 0.0001 MOI and isoniazid at 10 mg/L and **(B)** the 3-phage cocktail at 0.0001 MOI and rifampicin at 10 mg/L, where **(i)** represents absorbance @ 600 nm vs. time **(ii)** represents Log_{10}CFU/mL vs. time. The black arrow represents the time when phage solution and antibiotics were added to the cultures. The dashed green line indicates the limit of detection. These experiments were repeated twice (with $n = 3$), and the representative results are shown here. 2-way ANOVA with Tukey's multiple comparisons test was used to determine statistical significance ($p < 0.05$). Statistics data are represented in Tables S3 and S4.

Mycobacterium abscessus infection using a three-phage cocktail intravenously underscores their therapeutic potential [23]. Similarly, Little et al. reported a successful treatment of an immunocompromised individual with a chronic disseminated *M. chelonae* infection using a combination of antimicrobial medications, surgical intervention, and single bacteriophage therapy. Despite the development of neutralizing antibodies against the

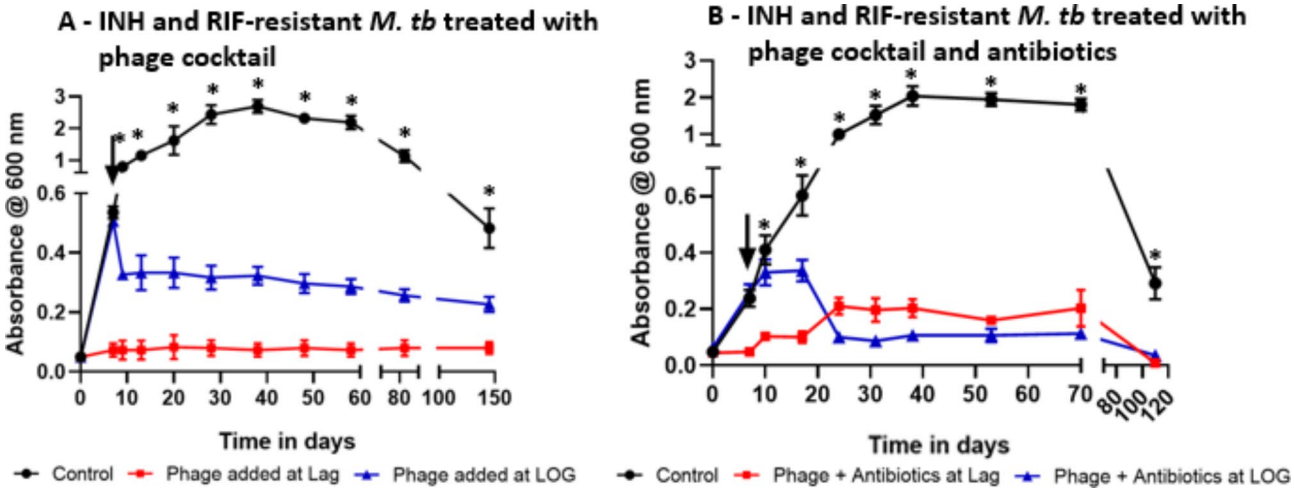

Fig. 6 Phage cocktails are effective against INH and RIF–resistant *M. tuberculosis* mc^2 8251. (**A**) Growth curves of *M. tuberculosis* in liquid culture in the presence of phage cocktail (D29, TM4, and DS6A). (**B**) Growth curves of *M. tuberculosis* in liquid culture in the presence of phage cocktail (D29, TM4, and DS6A) and antibiotics – isoniazid (INH at 1 mg/L) and rifampicin (RIF 4 mg/L). The black arrow represents the time when phage solution was added to the cultures. The experiment with only phage cocktail treatment (**A**) was repeated twice (with $n = 3$), and the representative graphs were plotted. 2-way ANOVA with Tukey's multiple comparisons test was used to determine statistical significance ($p < 0.05$). * Indicates a significant difference ($p < 0.05$) between the control and phage groups.

bacteriophage, the patient exhibited stable improvement with no bacterial resistance [43].

In our study, we investigated the efficacy of mycobacteriophages against *M. tuberculosis*, emphasizing factors such as the multiplicity of infection (MOI) and dosing regimen. Surprisingly, we found that mycobacteriophages could effectively infect and lyse *M. tuberculosis* cultures in vitro, even at low MOIs of 0.001 during the log phase and 0.0001 during the lag phase. To our knowledge, this is the first report demonstrating prolonged efficacy of phages at such low MOIs in *M. tuberculosis*. This contrasts with our earlier findings with *M. smegmatis*, where phages were effective at an MOI of 10 or more, possibly due to higher phage receptor abundance or greater affinity for phages in *M. tuberculosis* [29]. *M. tuberculosis's* slower replication rate (18–24 h) allows phages to initiate bursting within 3–4 h after infection, with varying burst sizes (see Supplementary Fig. 4), while *M. smegmatis* (replicating every 3–4 h) experiences phage bursting within 1–2 h, which is close with the timeframe of observed [44]. This slower replication of *M. tuberculosis* enables phages to replicate multiple times and infect bacteria before they complete their replication cycle. Additionally, differences in phage-defense systems between the two species could also contribute to variations in the MOI required to effectively reduce bacterial growth.

Multiple phage resistance mechanisms have been reported that can emerge during phage treatment [45, 46]. While a few phage resistance mechanisms are known in *M. tuberculosis*, such as specific mutations in loci Rv1043C and Rv1712 resulting in resistance to certain phages, adaptive CRISPR-mediated immunity has not been observed [47]. *M. tuberculosis* also has toxin-antitoxin systems that may play a role in viral defense [44, 48]. Our study found no genetic phage resistance in phage-treated *M. tuberculosis* cultures. Instead, we observed a phenotypic tolerance mechanism observed as biofilm-like aggregates, rich in cellulose, DNA, and proteins which protect against phages (Fig. 2A-D). This remarkable observation represents, to our knowledge, the first reported instance of phage tolerance in *M. tuberculosis* through biofilm-like morphology observed in vitro, complementing previous reports of biofilm formation by *M. tuberculosis* and the presence of cellulose components in these biofilms in vivo [33, 38].

In contrast, using a three-phage (D29, TM4 and DS6A) cocktail for treatment, we observed sustained efficacy with no regrowth observed for up to 100 days (Fig. 3), consistent with studies supporting the effectiveness of phage cocktails in minimizing resistance development [49–52].

Given that *M. tuberculosis* resides within granulomas, creating hypoxic conditions during infection, we tested phage efficacy under hypoxia [53]. Phages successfully infected and killed *M. tuberculosis* under these conditions (Fig. 4A).

To mimic the intracellular environment in phagocytic cells like macrophages, we conducted a phage infection study under acidic pH conditions in the presence of host-relevant carbon sources like Oleic Acid and Cholesterol. Mycobacteriophages exhibited remarkable efficiency in infecting and killing *M. tuberculosis* even under acidic pH (Fig. 4B). However, in vivo, the phages must penetrate macrophages and engage with bacteria to exert their

efficacy. The delivery of mycobacteriophages to intracellular compartments and inside granuloma can be challenging, and researchers have explored various strategies to achieve this goal [21, 54–56].

Our study examined the efficiency of two frontline drugs used to combat this complex disease pathology. After treatment with rifampicin (at 2 mg/L) or isoniazid (at 10 mg/L), the cultures regrew after 15 days. Additionally, we investigated the efficiency of phages in combination with these antibiotics (Fig. 5). We observed that during the lag phase, the phages and antibiotic co-treated group exhibited efficiency similar to the phage-only group. However, we did not observe synergy or additive effects when treated during the log phase, aligning with the reported phage-inhibiting effects of rifampicin and isoniazid (Fig. 5, Table S4) [57].

Our study also evaluated phage infection in MDR *M. tuberculosis* strains, showing that phages effectively eliminated the bacteria, both with and without antibiotics, with no regrowth observed (Fig. 6). Our findings highlight the potential of phage therapy for drug-resistant TB, aligning with promising outcomes from previous studies on *Mycobacterium abscessus* infections [23–26]. This study significantly adds to our understanding of phage therapy's potential in addressing drug-resistant infections and suggests that phages have the potential to be used along with antibiotics to treat drug-resistant TB.

Considering the complex disease pathology involving bacterial survival in low pH and hypoxia, direct interaction with bacteria is vital for phage effectiveness. Overcoming challenges such as efficient phage delivery within infected mammalian cells and managing potential immune responses, including neutralizing antibodies [58], is imperative. It's also crucial to recognize that mycobacteriophages exhibit high specificity, necessitating future testing on large number of clinical MDR strains. Addressing these challenges in future studies is essential for advancing the efficacy of phage therapy for tuberculosis.

Conclusions

Our results show that phage cocktails are effective against *M. tuberculosis* at low MOI and under various pathophysiological conditions. We also found a lack of synergy with antibiotics for antibiotic-susceptible strains, while the cocktails remained effective against drug-resistant strains of *M. tuberculosis*. These results show the potential of phages in developing treatments to combat antibiotic-resistant *M. tuberculosis* infections.

Abbreviations

BSL	Bio-Safety Level
CFU	Colony-Forming Unit
INH	Isoniazid
MOI	Multiplicity of Infection
MDR	Multi-drug Resistant
M. tuberculosis	*Mycobacterium tuberculosis*
OD	Optical Density
Phage	Bacteriophage
RIF	Rifampicin
TB	Tuberculosis

Supplementary Information

The online version contains supplementary material available at https://doi.org/10.1186/s12866-024-03474-3.

Supplementary Material 1

Acknowledgements

We acknowledge Dr. Graham Hatfull (University of Pittsburgh) and Dr. Sujoy K. Dasgupta (Bose Institute, Kolkata) for providing us with mycobacteriophages. We acknowledge Dr. Amit Singh (Indian Institute of Science, Bengaluru) for providing *M. tuberculosis* H37Rv wild-type bacterial strain. We acknowledge Dr. Willian R. Jacob Jr. (Albert Einstein College of Medicine) for providing us with the M. tuberculosis mc28251 strain. We are grateful to the Centre for Infectious Diseases Research (CIDR) at IISc Bangalore for allowing us to conduct studies in the Biosafety Level-3 facility. We thank Dr. Vijaya and Rajagopal Rao for funding Biomedical Engineering research at the Department of Bioengineering (BE). BSL-3 facility, AFMM facility, BE Imaging facility and BE central facility are also acknowledged for access to various instruments.

Author contributions

Sharumathi Jeyasankar: Conceptualization, Methodology, Data curation, Formal analysis, Validation, Visualization, Writing – Original draft. Yeswanth Chakravarthy Kalapala: Methodology and Data curation, Formal analysis, Validation. Pallavi Raj Sharma: Data acquisition. Rachit Agarwal: Conceptualization, Funding acquisition, Supervision, Writing – Original draft. All authors reviewed and approved the final version of the manuscript.

Funding

This work was supported by the Bill & Melinda Gates Foundation [OPP1210498].

Data availability

All the data presented by this study have been submitted with this research paper. Raw data and any other forms data generated by this research can be obtained from the corresponding author upon request by e-mail.

Declarations

Ethics approval

Experiments involving *Mycobacterium tuberculosis* were performed in a Biosafety level-3 facility (Institutional Biosafety Committee approval: IBSC/IISc/RA/20/2020).

Consent to participate

Not applicable.

Consent for publication

Not applicable.

Competing interests

The authors declare no competing interests.

Received: 15 July 2024 / Accepted: 23 August 2024
Published online: 04 September 2024

References

1. Hershkovitz I, Donoghue HD, Minnikin DE, Besra GS, Lee OYC, Gernaey AM et al. Detection and Molecular Characterization of 9000-Year-Old

Mycobacterium tuberculosis from a Neolithic Settlement in the Eastern Mediterranean. Ahmed N, editor. PLoS ONE. 2008;3(10):e3426.
2. Global Tuberculosis Report. 2023 [Internet]. [cited 2024 Feb 7]. https://www.who.int/teams/global-tuberculosis-programme/tb-reports/global-tuberculosis-report-2023
3. Verschoor JA, Baird MS, Grooten J. Towards understanding the functional diversity of cell wall mycolic acids of Mycobacterium tuberculosis. Prog Lipid Res. 2012;51(4):325–39.
4. Hett EC, Rubin EJ. Bacterial growth and cell division: a mycobacterial perspective. Microbiol Mol Biol Rev MMBR. 2008;72(1):126–56.
5. Liu CH, Liu H, Ge B. Innate immunity in tuberculosis: host defense vs pathogen evasion. Cell Mol Immunol. 2017;14(12):963–75.
6. Awuh JA, Flo TH. Molecular basis of mycobacterial survival in macrophages. Cell Mol Life Sci. 2017;74(9):1625–48.
7. Chai Q, Wang L, Liu CH, Ge B. New insights into the evasion of host innate immunity by Mycobacterium tuberculosis. Cell Mol Immunol. 2020;17(9):901–13.
8. Bussi C, Gutierrez MG. Mycobacterium tuberculosis infection of host cells in space and time. FEMS Microbiol Rev. 2019;43(4):341–61.
9. WHO consolidated guidelines on tuberculosis. Module 4: treatment - drug-resistant tuberculosis treatment, 2022 update [Internet]. [cited 2023 Jul 4]. https://www.who.int/publications-detail-redirect/9789240063129
10. Labuda SM, Seaworth B, Dasgupta S, Goswami ND. Bedaquiline, pretomanid, and linezolid with or without moxifloxacin for tuberculosis. Lancet Respir Med. 2024;12(2):e5–6.
11. Xia H, Zheng Y, Liu D, Wang S, He W, Zhao B, et al. Strong increase in Moxifloxacin Resistance Rate among Multidrug-Resistant Mycobacterium tuberculosis isolates in China, 2007 to 2013. Microbiol Spectr. 2021;9(3):e00409–21.
12. Mallick JS, Nair P, Abbew ET, Van Deun A, Decroo T. Acquired bedaquiline resistance during the treatment of drug-resistant tuberculosis: a systematic review. JAC-Antimicrob Resist. 2022;4(2):dlac029.
13. Nambiar R, Tornheim JA, Diricks M, Bruyne KD, Sadani M, Shetty A, et al. Linezolid resistance in Mycobacterium tuberculosis isolates at a tertiary care centre in Mumbai, India. Indian J Med Res. 2021;154(1):85.
14. Allué-Guardia A, Saranathan R, Chan J, Torrelles JB. Mycobacteriophages as potential therapeutic agents against drug-resistant tuberculosis. Int J Mol Sci. 2021;22(2):735.
15. Hatfull GF, Mycobacteriophages. Microbiol Spectr. 2018;6(5). https://doi.org/10.1128/microbiolspec.gpp3-0026-2018.
16. Guerrero-Bustamante CA, Dedrick RM, Garlena RA, Russell DA, Hatfull GF. Toward a phage cocktail for tuberculosis: susceptibility and Tuberculocidal Action of mycobacteriophages against Diverse Mycobacterium tuberculosis strains. mBio. 2021;12(3). https://doi.org/10.1128/mbio.00973.
17. Hatfull GF, Hendrix RW. Bacteriophages and their genomes. Curr Opin Virol. 2011;1(4):298–303.
18. Jacobs-Sera D, Marinelli L, Bowman C, Broussard G, Guerrero C, Boyle M, et al. On the nature of mycobacteriophage diversity and host preference. Virology. 2012;434(2):187–201.
19. Carrigy NB, Chang RY, Leung SSY, Harrison M, Petrova Z, Pope WH, et al. Anti-tuberculosis bacteriophage D29 delivery with a vibrating Mesh Nebulizer, Jet Nebulizer, and Soft Mist Inhaler. Pharm Res. 2017;34(10):2084–96.
20. Carrigy NB, Larsen SE, Reese V, Pecor T, Harrison M, Kuehl PJ, et al. Prophylaxis of Mycobacterium tuberculosis H37Rv infection in a Preclinical Mouse Model via Inhalation of Nebulized Bacteriophage D29. Antimicrob Agents Chemother. 2019;63(12):e00871–19.
21. Broxmeyer L, Sosnowska D, Miltner E, Chacón O, Wagner D, McGarvey J, et al. Killing of Mycobacterium avium and Mycobacterium tuberculosis by a Mycobacteriophage delivered by a nonvirulent Mycobacterium: a model for phage therapy of intracellular bacterial pathogens. J Infect Dis. 2002;186(8):1155–60.
22. Yang F, Labani-Motlagh A, Bohorquez JA, Moreira JD, Ansari D, Patel S, et al. Bacteriophage therapy for the treatment of Mycobacterium tuberculosis infections in humanized mice. Commun Biol. 2024;7(1):1–13.
23. Dedrick RM, Guerrero-Bustamante CA, Garlena RA, Russell DA, Ford K, Harris K, et al. Engineered bacteriophages for treatment of a patient with a disseminated drug-resistant Mycobacterium abscessus. Nat Med. 2019;25(5):730–3.
24. Nick JA, Dedrick RM, Gray AL, Vladar EK, Smith BE, Freeman KG, et al. Host and pathogen response to bacteriophage engineered against Mycobacterium abscessus lung infection. Cell. 2022;185(11):1860–e187412.
25. Dedrick RM, Freeman KG, Nguyen JA, Bahadirli-Talbott A, Cardin ME, Cristinziano M, et al. Nebulized bacteriophage in a patient with refractory Mycobacterium abscessus lung disease. Open Forum Infect Dis. 2022;9(7):ofac194.
26. Dedrick RM, Smith BE, Cristinziano M, Freeman KG, Jacobs-Sera D, Belessis Y, et al. Phage therapy of Mycobacterium infections: compassionate use of phages in 20 patients with drug-resistant mycobacterial disease. Clin Infect Dis. 2023;76(1):103–12.
27. Lenaerts A, Barry CE, Dartois V. Heterogeneity in tuberculosis pathology, microenvironments and therapeutic responses. Immunol Rev. 2015;264(1):288–307.
28. Korb VC, Chuturgoon AA, Moodley D. Mycobacterium tuberculosis: manipulator of protective immunity. Int J Mol Sci. 2016;17(3):131.
29. Kalapala YC, Sharma PR, Agarwal R. Antimycobacterial Potential of Mycobacteriophage Under Disease-Mimicking Conditions. Front Microbiol [Internet]. 2020 [cited 2023 Jun 27];11. https://www.frontiersin.org/articles/https://doi.org/10.3389/fmicb.2020.583661
30. Sarkis GJ, Hatfull GF, Mycobacteriophages. Methods Mol Biol Clifton NJ. 1998;101:145–73.
31. Kuru E, Hughes HV, Brown PJ, Hall E, Tekkam S, Cava F, et al. In situ probing of newly synthesized Peptidoglycan in live Bacteria with fluorescent D-Amino acids. Angew Chem Int Ed. 2012;51(50):12519–23.
32. Baranowski C, Welsh MA, Sham LT, Eskandarian HA, Lim HC, Kieser KJ et al. Maturing Mycobacterium smegmatis peptidoglycan requires non-canonical crosslinks to maintain shape. Garrett WS, Kana BD, Arthur M, editors. eLife. 2018;7:e37516.
33. Trivedi A, Mavi PS, Bhatt D, Kumar A. Thiol reductive stress induces cellulose-anchored biofilm formation in Mycobacterium tuberculosis. Nat Commun. 2016;7(1):11392.
34. Gouzy A, Healy C, Black KA, Rhee KY, Ehrt S. Growth of Mycobacterium tuberculosis at acidic pH depends on lipid assimilation and is accompanied by reduced GAPDH activity. Proc Natl Acad Sci. 2021;118(32):e2024571118.
35. Sumitani M, Takagi S, Tanamura Y, Inoue H. Oxygen Indicator Composed of an Organic/Inorganic hybrid compound of Methylene Blue, reductant, surfactant and Saponite. Anal Sci. 2004;20(8):1153–7.
36. Boshoff HIM, Myers TG, Copp BR, McNeil MR, Wilson MA, Barry CE. The transcriptional responses of Mycobacterium tuberculosis to inhibitors of metabolism: NOVEL INSIGHTS INTO DRUG MECHANISMS OF ACTION *. J Biol Chem. 2004;279(38):40174–84.
37. Vilchèze C, Copeland J, Keiser TL, Weisbrod T, Washington J, Jain P, et al. Rational design of Biosafety Level 2-Approved, Multidrug-resistant strains of Mycobacterium tuberculosis through Nutrient Auxotrophy. mBio. 2018;9(3):e00938–18.
38. Chakraborty P, Bajeli S, Kaushal D, Radotra BD, Kumar A. Biofilm formation in the lung contributes to virulence and drug tolerance of Mycobacterium tuberculosis. Nat Commun. 2021;12(1):1606.
39. Calcuttawala F, Shaw R, Sarbajna A, Dutta M, Sinha S, Gupta SKD. Apoptosis like symptoms associated with abortive infection of Mycobacterium smegmatis by mycobacteriophage D29. PLoS ONE. 2022;17(5):e0259480.
40. Abedon ST. Lysis from without. Bacteriophage. 2011;1(1):46–9.
41. Khawbung JL, Nath D, Chakraborty S. Drug resistant tuberculosis: a review. Comp Immunol Microbiol Infect Dis. 2021;74:101574.
42. Singh A, Prasad R, Balasubramanian V, Gupta N. Drug-resistant tuberculosis and HIV infection: current perspectives. HIVAIDS Auckl NZ. 2020;12:9–31.
43. Little JS, Dedrick RM, Freeman KG, Cristinziano M, Smith BE, Benson CA, et al. Bacteriophage treatment of disseminated cutaneous Mycobacterium chelonae infection. Nat Commun. 2022;13(1):2313.
44. Ramage HR, Connolly LE, Cox JS. Comprehensive Functional Analysis of Mycobacterium tuberculosis Toxin-Antitoxin systems: implications for Pathogenesis, stress responses, and evolution. PLoS Genet. 2009;5(12):e1000767.
45. El Haddad L, Harb CP, Gebara MA, Stibich MA, Chemaly RF. A systematic and critical review of bacteriophage therapy against Multidrug-resistant ESKAPE organisms in humans. Clin Infect Dis. 2019;69(1):167–78.
46. Oechslin F. Resistance Development to bacteriophages occurring during bacteriophage therapy. Viruses. 2018;10(7):351.
47. Diacon AH, Guerrero-Bustamante CA, Rosenkranz B, Rubio Pomar FJ, Vanker N, Hatfull GF. Mycobacteriophages to treat tuberculosis: dream or Delusion? Respiration. 2022;101(1):1–15.
48. LeRoux M, Laub MT. Toxin-antitoxin systems as Phage Defense Elements. Annu Rev Microbiol. 2022;76(1):21–43.
49. Fischer S, Kittler S, Klein G, Glünder G. Impact of a single phage and a phage cocktail application in broilers on reduction of Campylobacter jejuni and development of resistance. PLoS ONE. 2013;8(10):e78543.
50. Yang Y, Shen W, Zhong Q, Chen Q, He X, Baker JL et al. Development of a Bacteriophage Cocktail to Constrain the Emergence of Phage-Resistant Pseudomonas aeruginosa. Front Microbiol [Internet]. 2020 [cited 2024 Feb

8];11. https://www.frontiersin.org/journals/microbiology/articles/https://doi.org/10.3389/fmicb.2020.00327
51. Gao D, Ji H, Wang L, Li X, Hu D, Zhao J, et al. Fitness Trade-Offs in Phage Cocktail-Resistant Salmonella enterica Serovar Enteritidis results in increased antibiotic susceptibility and reduced virulence. Microbiol Spectr. 2022;10(5):e0291422.
52. Borin JM, Lee JJ, Gerbino KR, Meyer JR. Comparison of bacterial suppression by phage cocktails, dual-receptor generalists, and coevolutionarily trained phages. Evol Appl. 2022;16(1):152–62.
53. Ehlers S, Schaible UE. The Granuloma in Tuberculosis: Dynamics of a Host–Pathogen Collusion. Front Immunol [Internet]. 2013 Jan 7 [cited 2024 Jul 6];3. https://www.frontiersin.org/journals/immunology/articles/https://doi.org/10.3389/fimmu.2012.00411/full
54. Danelishvili L, Young LS, Bermudez LE. In vivo efficacy of phage therapy for Mycobacterium avium infection as delivered by a nonvirulent mycobacterium. Microb Drug Resist Larchmt N. 2006;12(1):1–6.
55. Sweeney KA, Dao DN, Goldberg MF, Hsu T, Venkataswamy MM, Henao-Tamayo M, et al. A recombinant Mycobacterium smegmatis induces potent bactericidal immunity against Mycobacterium tuberculosis. Nat Med. 2011;17(10):1261–8.
56. Nieth A, Verseux C, Barnert S, Süss R, Römer W. A first step toward liposome-mediated intracellular bacteriophage therapy. Expert Opin Drug Deliv. 2015;12(9):1411–24.
57. Li X, He Y, Wang Z, Wei J, Hu T, Si J, et al. A combination therapy of phages and antibiotics: two is better than one. Int J Biol Sci. 2021;17(13):3573–82.
58. Dedrick RM, Freeman KG, Nguyen JA, Bahadirli-Talbott A, Smith BE, Wu AE, et al. Potent antibody-mediated neutralization limits bacteriophage treatment of a pulmonary Mycobacterium abscessus infection. Nat Med. 2021;27(8):1357–61.

Publisher's note